

DEVELOPMENT OF FASTENER MODELS FOR IMPACT SIMULATION OF COMPOSITE STRUCTURES

Andrew J. Gunnion*, Hannes Körber**, David J. Elder*, Rodney S. Thomson*

*Cooperative Research Centre for Advanced Composite Structures Limited
506 Lorimer Street Fishermans Bend, Victoria, 3207, Australia

**University of Stuttgart, Germany

Keywords: *composite materials, fasteners, impact, simulation*

Abstract

High energy impact, such as bird-strike, is an important consideration in the design of aircraft structures. Although advanced numerical simulation is increasingly being used by aircraft designers to model impact events, further research into the behaviour of materials and joints is required to develop improved numerical models. The damage and failure behaviour of fastened composite joints, critical to the overall response of a structure under impact, is investigated through experiment and simulation. An existing fastener model suitable for modelling composite joints in impact simulation was evaluated and found to perform adequately, however more development is required to accurately capture all aspects of fastener failure in composites and the resulting damage in the structure.

1 Introduction

1.1 Impact Simulation

High energy impact, such as bird-strike, can cause significant damage to wing leading and trailing edge devices. Where such devices are critical to the safe operation of the aircraft, they must be designed to withstand possible impact damage. Historically, impact damage was accounted for in design by assuming a certain damage size. One such method is to create a hole through the structure, as if the bird punches through on impact. Critical components may

then be tested for certification using real or synthetic birds fired at high speed from a pneumatic gun. Although this approach may develop an impact-resistance structure, it is costly and will likely result in an overly-conservative design, adding extra weight and cost to the product. Furthermore, it is possible that the bird-strike may introduce high reaction loads and other damage modes that are not captured by this method.

For this and many other similar design problems, advanced numerical simulation methods, in conjunction with robust validation, now provide aircraft designers an alternative to overly-conservative assumptions or large test programs. Impact and crash simulation is increasingly being used for the design of current and future generations of aircraft.

Although impact and crash analyses are already being used in aircraft design, and have been extensively used in the automotive industry, there remain numerous areas where further understanding of the underlying physical behaviour is required. Armed with this knowledge, improved models for materials, joints, contact, and other aspects of impact and crash simulation can be developed. To this end, several international research programs have recently investigated many aspects specifically relating to simulation of bird-strike on aircraft structures [1-3], but further development is still required.

1.2 Fastened Joints in Composite Structures

Fastened composite joints is one area where further understanding of the failure and damage

mechanisms is required to improve the accuracy of joint models used in crash and impact simulations. For normal aircraft design purposes, fastened joint behaviour up to the point of failure is sufficient. For impact and crash analysis, the behaviour of joints beyond initial failure and up to complete separation is required.

Past research has been performed into detailed analyses of fasteners that use hundreds of solid elements, nonlinear material models and contact algorithms [4-5]. While detailed local models may lead to a better understanding of joint failure, improved fastener design and reduced experimental testing, they are not suitable for use in large-scale modelling of fastened structures. For simulation of impact on aircraft components, more efficient modelling techniques are required. Point link elements, or spot weld elements, offered by commercial explicit FE codes provide a convenient way to model a fastened joint.

1.3 Aim

In this paper, an experimental investigation into the damage and failure of composite fastened joints is documented, and the existing PLINK element available in Pam-Crash explicit finite element (FE) software is evaluated.

2 Aspects of Fasteners in Composites

Carbon fibre reinforced polymers (CFRP) make up a significant portion of civil and military aircraft structures. For next-generation civil airliners, such as the Airbus A380 and Boeing 787, it is claimed that composites, primarily CFRP, will constitute 22% and 50% of structural weight, respectively. The choices for joint design, being bonded, bolted or a combination of both [6], will likely remain unchanged for the foreseeable future, particularly for composite-to-metal joints.

From a structural efficiency perspective, bonded joints are preferable to bolted joints for composite structures as they provide a superior load path without damaging the composite by drilling. The maximum joint efficiency for a

bolted joint is 20-40% less in composites than for metals [7]. Bonded joints also offer significant potential savings during manufacture when compared to fastened joints because of the high cost of titanium fasteners (required to prevent galvanic corrosion when in contact with the carbon) and the time associated with drilling and installation. Yet for all the potential benefits of bonded joints in composites, bolted joints remain common place, particularly for primary structure, due to the limitations of current non-destructive inspection (NDI) technology and durability concerns. Bolted joints also offer some advantages where components need to be removed for inspection or maintenance during service.

The main failure modes of bolted composite joints that must be considered during design are shown in Figure 1. Through good design practise, often dictated by in-house design rules, the failure modes of a joint can be limited to bearing failure under shear loads and pull-through failure under tensile loads. For this reason, the experimental program developed for this investigation focused on these two common failure modes for bolted joints.

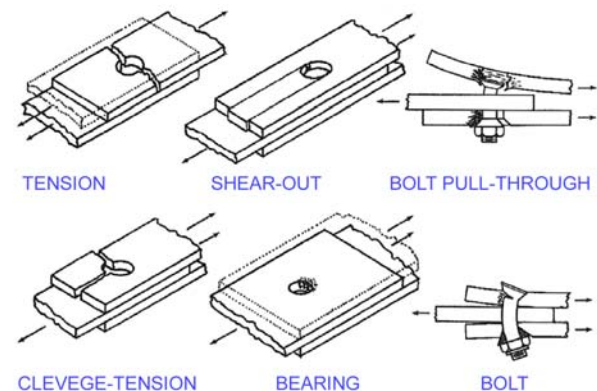


Fig 1. Failure modes in bolted composite joints, after [6]

Two main head types for mechanical fasteners used in aerospace structures are protruding head and countersunk head. Protruding head fasteners are used wherever possible as they ensure superior joint strength due to a larger bearing area and there is no damage caused to the composite as a result of the countersinking process. They are typically

limited to internal joints, such as cleats and around fittings. Countersunk fasteners are preferred wherever the fastener head is exposed to the free-stream for aerodynamic reasons. Hence, countersunk fasteners are used to join wing, tail and control-surface skins to the spars and ribs. As both countersunk and protruding head fasteners are widespread through aircraft structure, this investigation considers both head types and the different damage modes resulting from their failure. Furthermore, single-shear configurations, not double-shear as shown in Figure 1, will be investigated as this reflects typical aircraft assemblies.

3. Description of PLINK element

The PLINK is a penalty-based mass-less contact element available in Pam-Crash, suitable for modelling spotwelds, rivets and other discrete connections [8,9]. The PLINK element is a convenient way to model connections between segments (shell elements or faces of solids) because it is mesh-independent. A PLINK is generated within Pam-Crash by connecting segments within a given search radius of a reference node. The PLINK connectivity can be further constrained by defining a maximum length and number of layers to be joined. As the PLINK is mesh independent, the reference node need not be associated with any of the segments to be joined.

The effective stiffness of the resulting joint may vary depending on the PLINK connectivity. The user should ensure that the end fixity (fixed or pinned), normal stiffness and shear stiffness parameters combine to accurately reflect the stiffness of the joint being modelled. If required, the user can implement a nonlinear penalty stiffness to better model joint stiffness.

The most suitable PLINK options for modelling fasteners is to use force-based failure initiation coupled with displacement-based ultimate failure. This allows the model parameters to be calibrated to accurately reflect the energy absorbed during failure. The resulting force-displacement behaviour is shown in Figure 15, where D1 and D2 are the

displacement parameters. An interaction criterion is used to consider combined normal and shear loading, described by Equation 1.

$$\left(\frac{N}{N_U}\right)^a + \left(\frac{S}{S_U}\right)^b \geq 1 \quad (1)$$

where:

N, S Normal and shear load in the PLINK

N_U, S_U Ultimate normal and shear load

a, b Normal and shear weighting factors

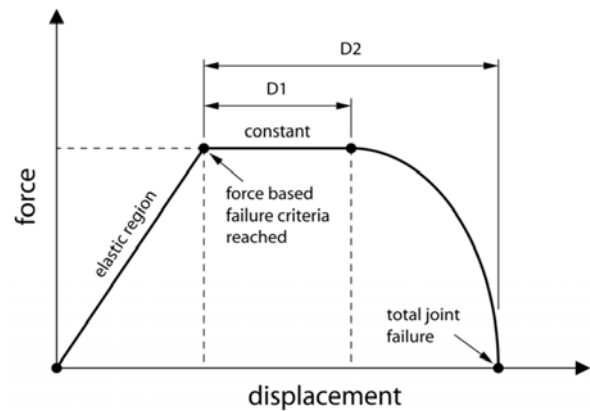


Fig 2. PLINK model load-displacement behaviour

4. Experimental Investigation

4.1 Aim

The aim of the experimental program was to investigate the stiffness, strength and damage behaviour of mechanically fastened CFRP joints representative of typical aircraft structures. Particular emphasis was placed on capturing the complete damage cycle to improve understanding of the damage mechanisms and energy absorbed during failure. These characteristics must be accurately modelled in impact and crash simulations but are not well documented from traditional tests that focus mainly on joint yield and ultimate strength.

4.2 Specimen Design

For this investigation, two different fastener configurations were investigated. Protruding head (PH) specimens used HiLok HL1012 pin

with HL1087 collar and the countersunk head (CS) specimens used HL523 pin with HL97 collar. The CFRP material used was CYCOM970 PWC T300 3K ST, a plain weave epoxy pre-preg with ply thickness of 0.22 mm. A symmetric, nominally quasi-isotropic lay-up was used in all specimens. A summary of the tested combinations of fastener type, diameter (d) and laminate thickness (t) investigated is given in Table 1 and Table 2 for the pull-through and shear tests respectively. For every tested combination of d and t , one specimen was unloaded and re-loaded to investigate the post-yielding stiffness. Recommended design practises [6,10] were used to ensure that ratios of t/d and h/d were satisfactory for each test condition, where h is the countersunk depth. These ratios are given by Equations 1 and 2. For this reason, no CS specimens were tested for the t_1 and d_1 combination.

$$\frac{t}{d} < 1 \quad (2)$$

$$\frac{h}{t} < 0.65 \quad (3)$$

4.3 Method

4.3.1 Pull-through Testing

For the loading of a bolted composite joint in the normal direction, little research has been done and no standard test procedure exists. Therefore, a test rig was designed to determine the pull-out loads of fasteners in composite laminates under a quasi-static tensile load condition based on recommendations given in [11,12]. The test rig, shown in Figure 3, has some unique features developed for this program:

- The ‘locking ring nut’ allows the operator to quickly interchange specimens without using any tools.
- Multiple ‘adaptor bushes’ with constant outer diameter but varying inner diameters allow rapid interchange of specimens with different fastener sizes.
- A pair of linear varying displacement transducers (LVDTs) placed under the specimen accurately record the displacement of the fastener head (LVDT1) and the surrounding laminate adjacent to the fastener (LVDT2).

The tests were performed using an INSTRON 5500R mechanical test machine with a maximum load of 100 kN. A constant loading rate of 1 mm/min was applied with data sampled at 1 Hz.

4.3.2 Shear Testing

When designing a composite joint, the preferred mode of failure for shear loading should be bearing of the fastener hole, to prevent catastrophic failure of the composite structure, thus following general design considerations given in [6,10]. The ASTM test standard D5961 [13] was chosen as a reference

Table 1. Pull-through test matrix showing number of specimens for each combination of d and t (mm)

PH \ CS	d_1	d_2	d_3
CS	3.97	4.76	6.35
t_1	5*	6	
2.42	0	5*	
t_2		6	6
3.52		6	6

*Indicates tests where unload-reload data was not recorded

Table 2. Shear test matrix showing number of specimens for each combination of d and t (mm)

PH \ CS	d_1	d_2	d_3
CS	3.97	4.76	6.35
t_1	5	5	
2.42	0	5	
t_2		5	5
3.52		5	5

for obtaining the bearing response as a result of shear loading of the single lap joint.

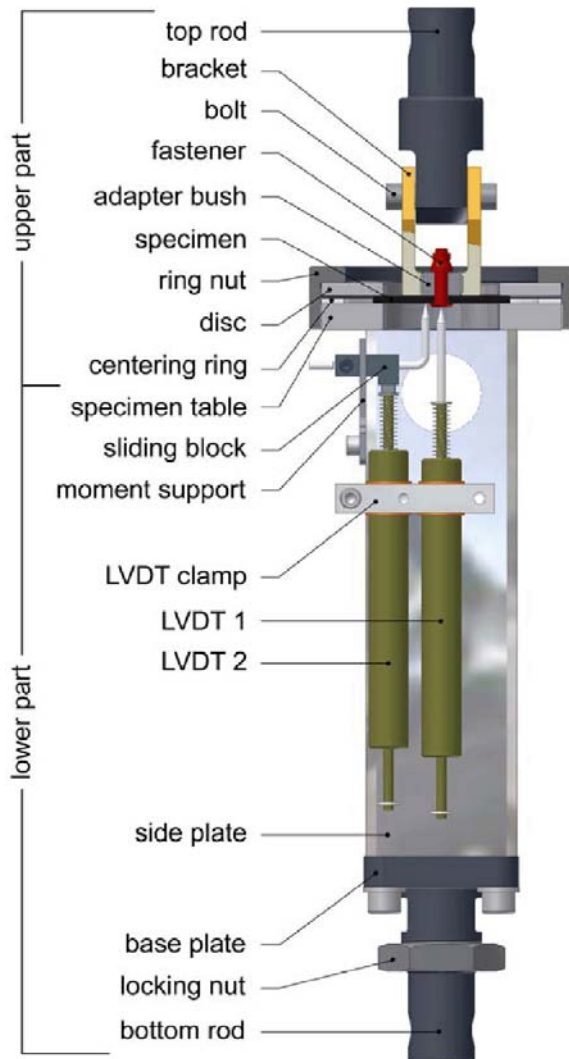


Fig 3. Test-rig designed to investigate fastener pull-through failure modes

It was initially intended to use an unsupported specimen. However, preliminary tests failed due to net tension, despite satisfying relevant design guidelines [6,10]. Therefore, it was decided to adopt a supported single-lap bearing test based on Procedure B of ASTM standard D 5961 [13]. The support fixture, shown in Figure 4, consists of six individual pieces (plus screws): two short grips, two long grips and two support plates. The single-lap specimen is placed between short and long

grips. Doublers are used to maintain the correct specimen geometry within the fixture.

Strain was measured by a face-mounted extensometer attached to the specimen. The tests were performed using an MTS hydraulic test machine with a maximum load of 250 kN. Whilst the loads expected were below 100 kN, a larger hydraulic machine was required to achieve the necessary clamping pressure. A constant loading rate of 1 mm/min was applied and data sampled at 10 Hz.

4.4 Results

4.4.1 Pull-through Testing

The load-displacement behaviour was plotted for each specimen. Sample load-displacement curves are given in Figure 5 and Figure 6 showing the results for one PH and CS fastener configuration. It can be seen that excellent consistency was found within each test configuration. This lack of scatter was evident for each test configuration, indicating that the quality control of the test and specimen preparation was excellent. It was also clear from all results, and typified in Figure 5 and Figure 6, that the same trends existed across all test configuration. That is, a linear elastic region (governed primarily by the composite panel stiffness), followed by reduced stiffness as the fastener started to pull through the laminate before the load quickly reduced after reaching an ultimate value.

The unload-reload behaviour is shown in Figure 5 and Figure 6 for one specimen in each case. It can be seen that this behaviour could easily be described by a straight line from the point of unload to the origin. This behaviour needs to be further investigated by attempting multiple load re-load cycles on different specimens at different loads.

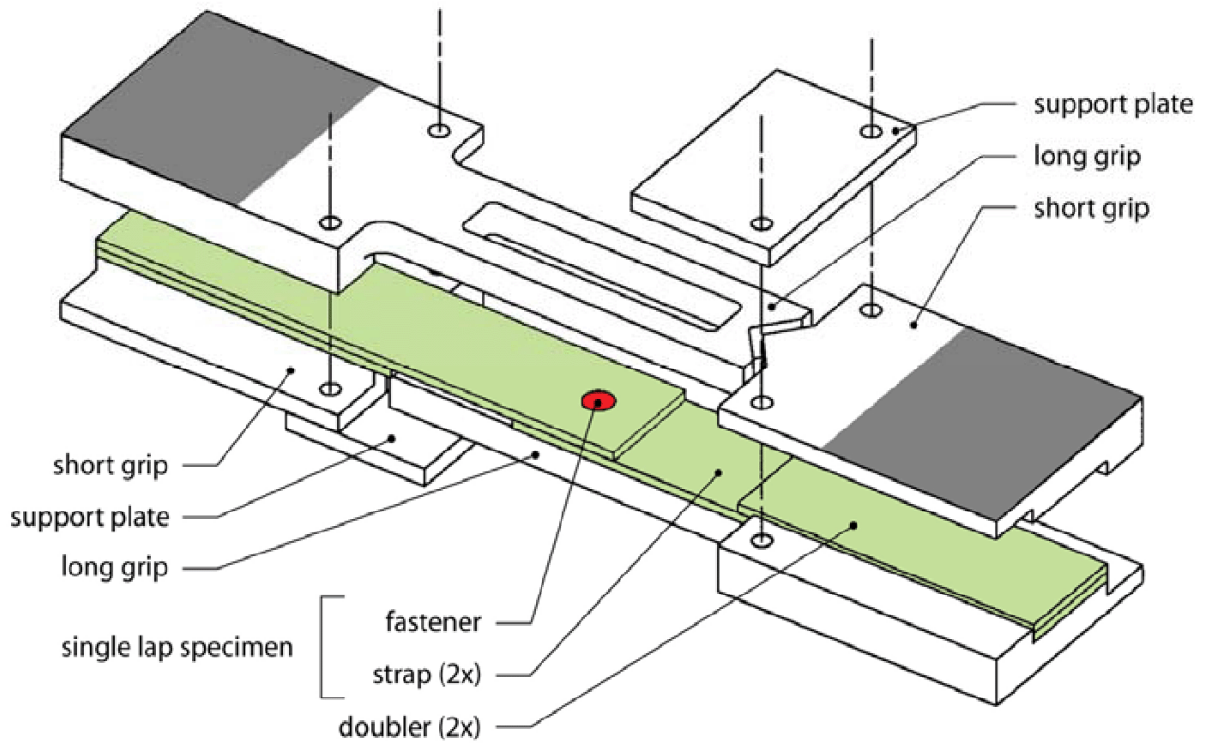


Fig 4. Shear test specimen and support fixture, after [11]

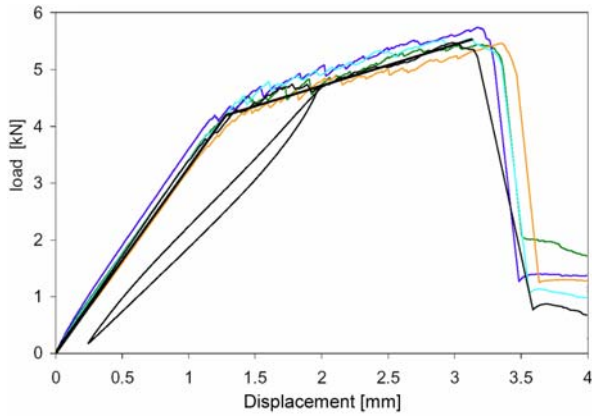


Fig 5. Pull-through load-displacement behaviour for PH d2 t2 specimens

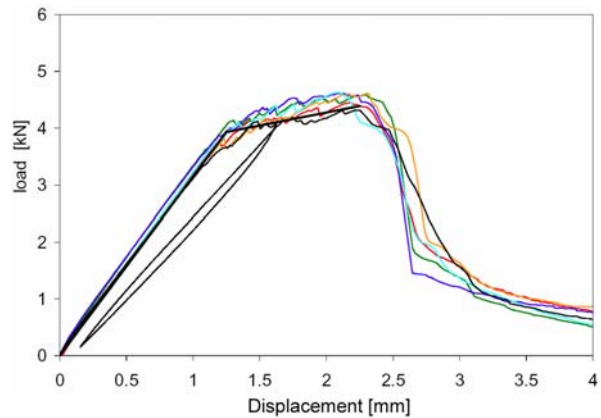


Fig 6. Pull-through load-displacement behaviour for CS d2 t2 specimens

In an attempt to remove the influence of fastener diameter and laminate thickness, a pull-through yield stress, σ_{Ny} , and ultimate stress σ_{Nu} , was calculated for the CS and PH fasteners using the Equation 4 and 5, where N_y and N_u are the yield and ultimate loads measured from the test, respectively.

$$\sigma_{Ny} = \frac{N_y}{dt} \quad (4)$$

$$\sigma_{Nu} = \frac{N_u}{dt} \quad (5)$$

The results are shown in Figure 7 and Figure 8, including error bars to indicate the maximum and minimum values from the test.

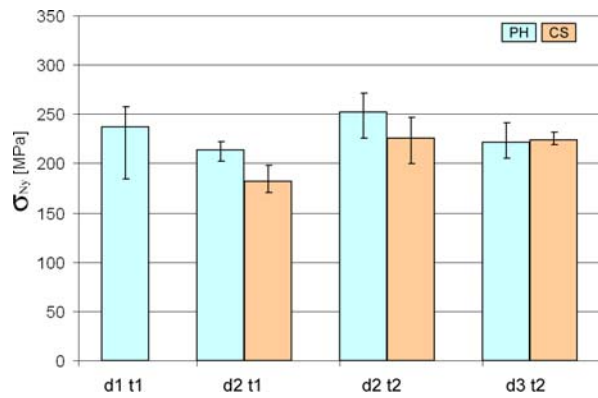


Fig 7. PH and CS average pull-through yield stress for various d and t combinations

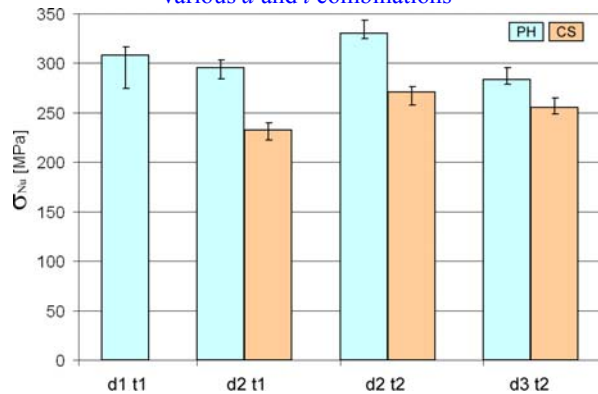


Fig 8. PH and CS average pull-through ultimate stress for various d and t combinations

A failed pull-through specimen is shown in Figure 9 for a CS fastener. A large hole can be seen from the top created by the fastener head. The specimen also delaminates as the fastener is pulled through the thickness. No failures of fasteners occurred.

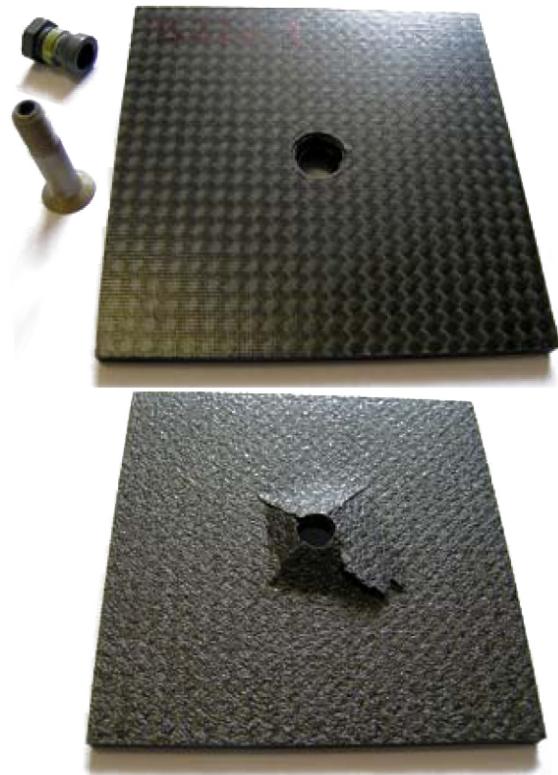


Fig 9. Failed specimen CS d2 t2 viewed from above and below after failure.

4.4.2 Shear Testing

The load-displacement behaviour of the shear tests was plotted for each specimen. Sample load-displacement curves are given in Figure 10 and Figure 11 showing the results for one PH and CS fastener configuration. As with the pull-through testing, excellent consistency was evident within each test configuration. However, unlike the pull-through test, it was also clear from all results, and typified in Figure 10 and Figure 11, that the same trends did not exist across all test configurations. The primary difference between the two head types was that the PH fasteners exhibited a sudden transition from the linear elastic to “plastic” regions while this transition was more gradual in the CS specimens.

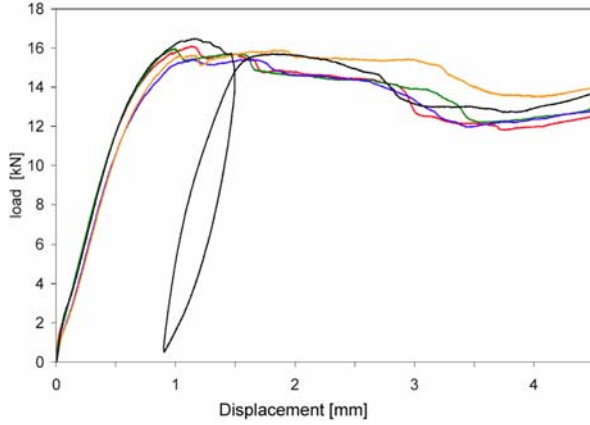


Fig 10. Shear load-displacement behaviour for PH d3 t2 specimens

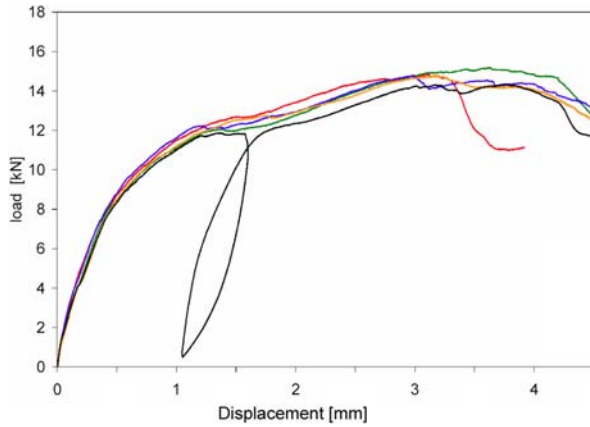


Fig 11. Shear load-displacement behaviour for CS d3 t2 specimens

The unload-reload behaviour is shown in Figure 10 and Figure 11 for one specimen in each case. It can be seen that this behaviour would be best described by a line parallel to the initial joint stiffness. This behaviour needs to be further investigated by attempting multiple load re-load cycles on different specimens at different loads.

In an attempt to remove the influence of fastener diameter and laminate thickness, a shear bearing yield stress, σ_{Sy} , and ultimate stress σ_{Su} , was calculated for the CS and PH fasteners using the Equation 6 and 7, where S_y and S_u are the yield and ultimate loads measured from the test, respectively. Determination of the yield load was not as simple as for the pull-through tests. A 0.2% strain offset approach was

employed, as described in ASTM test standard D5961 [13].

$$\sigma_{Sy} = \frac{S_y}{dt} \quad (6)$$

$$\sigma_{Su} = \frac{S_u}{dt} \quad (7)$$

The results are shown in Figure 12 and Figure 13, including error bars to indicate the maximum and minimum values from the test.

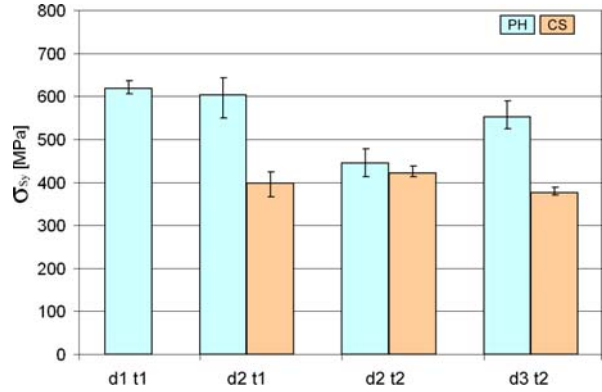


Fig 12. PH and CS average shear yield stress for various d and t combinations

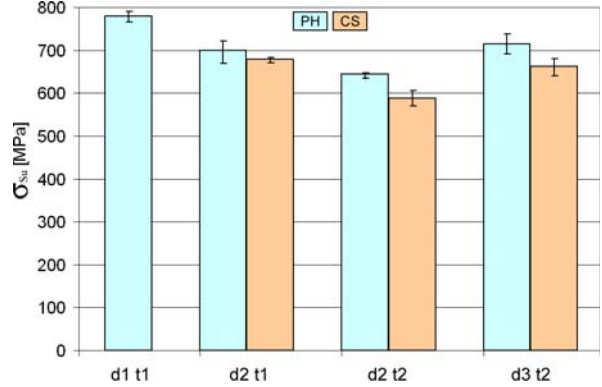


Fig 13. PH and CS average shear ultimate stress for various d and t combinations

Two failed shear specimens are shown in Figure 14. It can be seen that the fastener rotates under load and crushes the composite around the fastener head and collar. The differences in fastener geometry give rise to the different load-displacement curves seen in Figure 10 and 11.

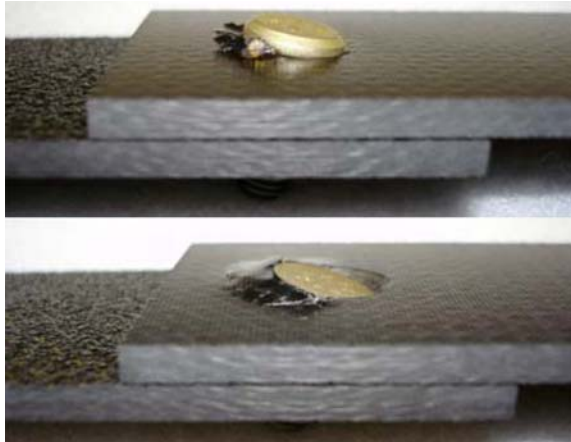


Fig 14. Damage evident in composite around fastener head for PH d3 t2 (top) and CS d3 t2 (bottom) specimens.

4.5 Discussion

The overall consistency of experimental results summarised in Figures 7, 8, 12 and 13 provide a good foundation from which methods for modelling fasteners can be evaluated.

The pull-through test results were very consistent. The load-displacement behaviour of all specimens can be described by Figure 15(a). The shear bearing specimens were not as consistent. Three different load-displacement trends were witnessed, two of which are evident in Figures 10 and 11. The three characteristic behaviours are summarised in Figure 15(b). This result suggests that the pull-through behaviour can be more easily captured in a simple model than the shear behaviour.

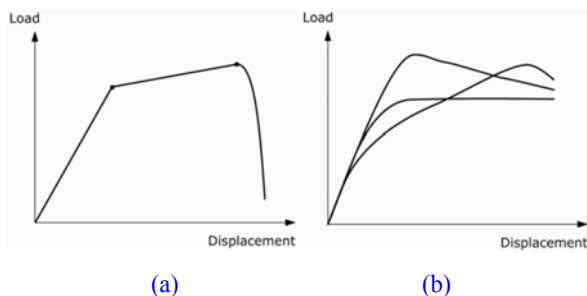


Fig 15. Idealised load-displacement behaviour from experiment for (a) pull-through and (b) shear

The unload-reload behaviour of the composite fastened joint loaded in pull-through and shear modes was also quite different, illustrated in Figure 16. Further experimental

testing is required at different load levels and for multiple reload cycles to fully characterise the two different modes shown, however the trends described in Figure 16 accurately reflect the experimental results of this program for all specimens tested.

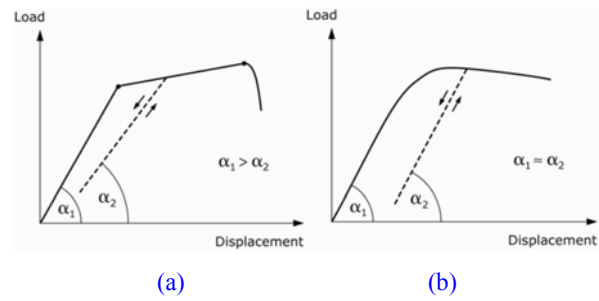


Fig 16. Idealised unload-reload behaviour from experiment for (a) pull-through and (b) shear

It was not possible to determine displacements corresponding to ultimate joint failure for the shear loading, however these displacements could be measured quite well for the pull-through tests. Average values for D1 and D2 were calculated from the experimental data for each fastener type to be used in the model.

5 Modelling Investigation

5.1 Aim

The aim of the modelling investigation was to evaluate the Pam-Crash PLINK element by attempting to simulate the experimental results reported in Section 4. Importantly, the model parameters used to simulate each test were determined in line with a practical design method, outlined in Section 5.2. The investigation was performed using the PLINK material type 302 in Pam-Crash 2003 [8,9]. A new PLINK material formulation is now available and will be evaluated in future work.

5.2 Model Parameters

When comparing the simulation and experiment result, best agreement would be achieved by using the unique material strength parameters

calculated from the experiment for each combination of d and t . However, this is not a practical method by which PLINK strengths can be determined when modelling large composite structures, where the number of d and t combinations is considerable. Instead, average values of pull-through and shear stresses determined from Equations 4 - 7 have been used to calculate the PLINK ultimate loads N_u and S_u .

A limitation of the current PLINK model is that the PLINK has no stiffness after reaching the ultimate force value, as shown in Figure 2. This does not reflect the experimental results for either the pull-through or shear loading where a clear change in stiffness was evident. A second limitation of the PLINK model is that the same D1 and D2 values apply to the pull-through and shear cases, yet the maximum displacement values are very different between the two modes. The PLINK model of Figure 2 can be made to fit the pull-through behaviour of Figure 15(a) far better than the shear behaviour, shown in Figure 15(b).

With the use of PLINK elements for crash and impact simulation in mind, the model parameters were developed to best represent the energy dissipated through both failure modes. That is, although the correlation between simulation and experiment could be improved by using different model parameters for the pull-through and shear cases, a single, set of parameters representing a compromise between the pull-through and shear behaviour was used to reflect the limitations of the PLINK when used in a large model where the loading is unknown.

The model parameters were determined from Equations 5 and 7. For N_u , the average of σ_{Ny} and σ_{Nu} was used to best reflect the energy absorbed. For S_u , σ_{Su} was used as many joint combinations tested exhibited little or no clear yielding region. The values of D1 and D2 were based on the average pull-through test results as no equivalent behaviour was evident from the bearing shear test, where the load remained constant for the duration of the applied displacement of 5 mm. This means that the energy dissipated in shear failure of the model will under-represent that observed in the test,

but reflects the current practical limitations of the PLINK. The weighting factors a and b (Equation 1) were assigned a value of 2 throughout this investigation. It was not possible to further refine the weighting parameters without access to suitable combined-loading test data. User-defined PLINK penalty stiffness values were not defined, leaving the PLINK stiffness to be determined by Pam-Crash.

In order to efficiently model the joints, the most critical failure mode of the joint likely to occur must be modelled. Assuming the joint has been well designed, these failure modes will be the pull-through and shear bearing as recreated in the tests described above. Whilst this approach is an efficient way to model a fastened composite joint, it must be realised that it is a simplification. Failure in a PLINK represents damage to the composite, not a fastener. This is particularly important when residual strength considerations are of concern, as the shell elements representing composite components in the model may not exhibit any damage, yet in reality, significant local laminate damage has occurred as a result of the fastened joint failure.

5.3 Pull-through Simulation

5.3.1 Model

The square laminate panel was modelled using shell elements. The upper and lower rings of the test rig were modelled with solid elements. A second plate represented the bracket which was joined to the composite specimen via a PLINK. A displacement load was then applied at a constant acceleration to the bracket. The composite specimen was allowed to slide inwards under load using a contact between the specimen and the disc and specimen table (refer Figure 3), which were modelled with rigid solid elements. The resulting FE model is shown in Figure 17. Element size was kept similar to that employed for larger impact model applications.

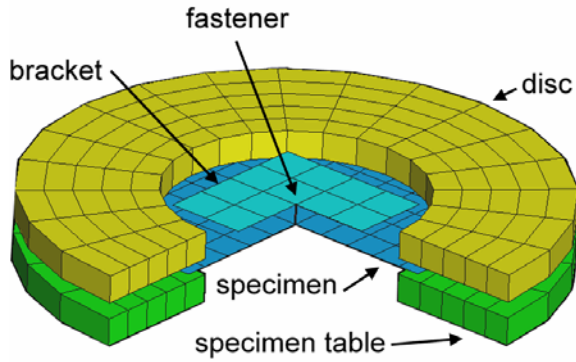


Fig 17. FE model for simulation pull-through tests; refer Figure 2

5.3.2 Results

The load-displacement from the pull-through simulation is plotted and compared with the trend-line from the test data in Figures 18 – 21. The load was recorded from the force required to lift the bracket. The displacement is that of LVDT1. To get an equivalent displacement in the model to that of LVDT1 from the test, the displacement of the panel centre node was used until the PLINK started to yield. At this point, the displacement of the bracket was used. This result simulates the fastener head first moving with the laminate, then through the laminate.

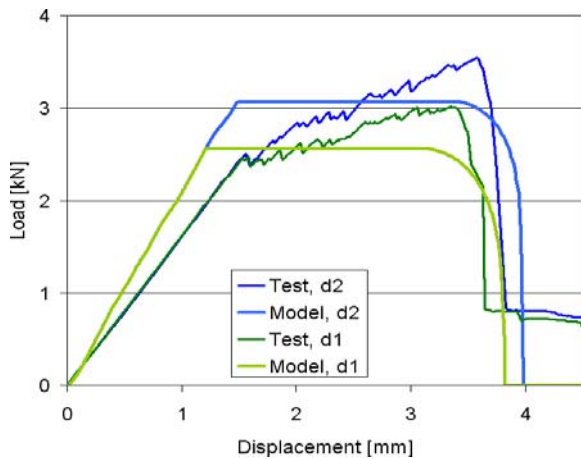


Fig 18. PLINK simulated pull-through force-displacement versus experimental result for PH fasteners, t1.

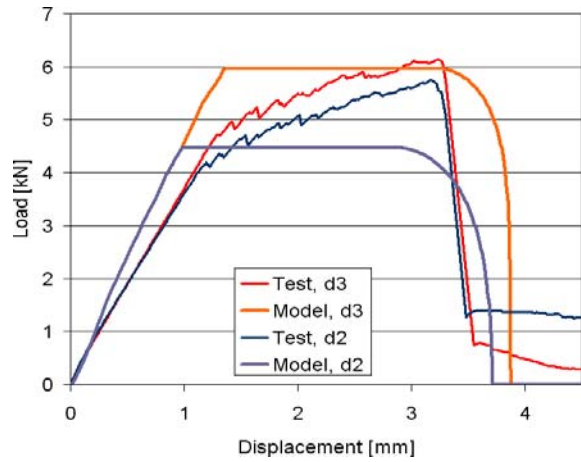


Fig 19. PLINK simulated pull-through force-displacement versus experimental result for PH fasteners, t2.

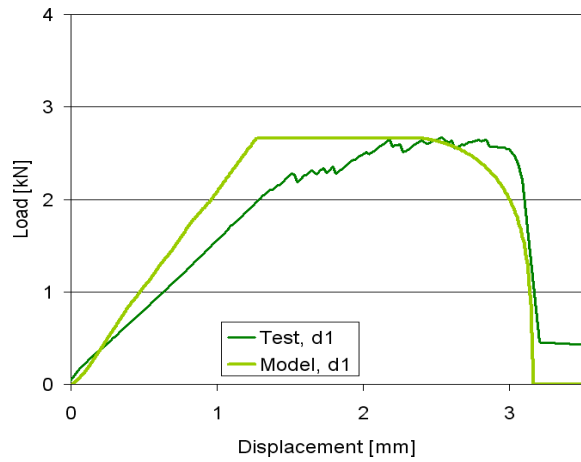


Fig 20. PLINK simulated pull-through force-displacement versus experimental result for CS fasteners, t1.

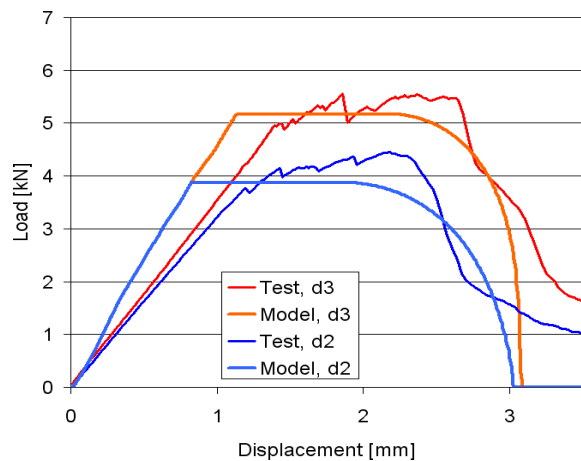


Fig 21. PLINK simulated pull-through force-displacement versus experimental result for CS fasteners, t2.

5.3.3 Discussion

It can be seen from Figures 18–21 that the pull-through model results correspond reasonably well to the experimental data.

For the pull-through case, the stiffness is dictated by the composite specimen, not the PLINK stiffness. Hence, the model predicts the same stiffness for a given panel thickness. In all comparisons, it can be seen that the simulated stiffness was greater than the test. One possible reason for this is that the model plate does not have a hole in the centre, which would have reduced the bending stiffness of the composite specimen in the test.

Small variations in ultimate load and displacement-to-failure were expected given the variations from the mean (refer Figures 7,8,12,13) which was used to develop the model parameters. Despite this variation, the overall response for all cases can be considered satisfactory.

5.4 Shear Simulation

5.4.1 Model

The shear bearing model was simpler than the pull-through model. The two composite plates were modelled with shell elements. No out-of-plane displacements were allowed within the plates to represent the restrictions imposed within the test fixture. A displacement load was then applied to one plate at a constant acceleration to simulate the test. Element size was kept similar to that employed for larger impact model applications.

Although the user can define a PLINK element independently of the mesh to be joined, the effective PLINK stiffness is connectivity dependant, particularly under shear loading. Two possible scenarios are illustrated in Figure 22, where the PLINK has matched nodes in the adjoining plates, and when the PLINK is offset between those nodes. For specimen PH d3 t2, the resulting load-displacement behaviour of the two modelling scenarios is shown in Figure 23 against the experimental trendline. It can be seen that the two methods give quite different stiffness. It can also be seen that the offset

PLINK model failure load corresponds to that used in the model, whereas the failure load of the matched model does not. For the case with matched nodes, the PLINK rotates significantly, resulting in a normal tensile force as well as a shear load. This results in the PLINK failing below the intended shear load due to the interaction criterion (Equation 1). As the offset model gives superior correlation to the test, it was used for all subsequent simulations.

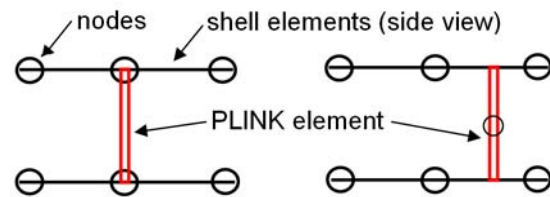


Fig 22. Two PLINK definition scenarios where the PLINK element is matched (left) or offset (right) from the nodes in the adjoining shells.

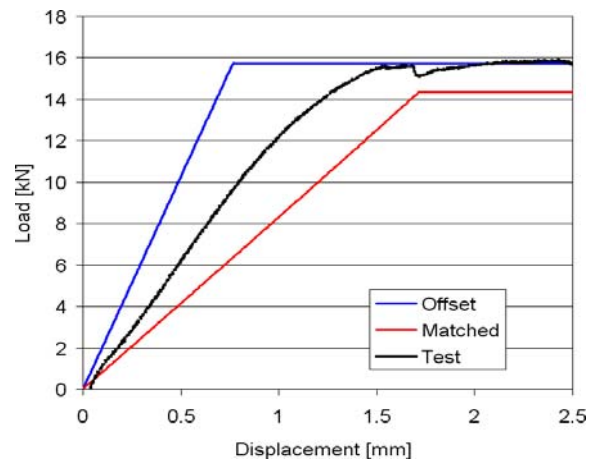


Fig 23. Comparison of load-displacement behaviour of PLINK with matched and offset positioning versus the experimental result for PH d3 t2.

5.4.2 Results

The load-displacement from the shear simulation is compared with the experimental result in Figures 24 – 27. As the experimental results showed excellent agreement for a given test configuration, a single representative test result is shown for each case. The load was recorded from the force required to displace one of the plates in the simulation. The displacement was measured as the relative displacement

between the plates, as recorded during the test by an extensometer.

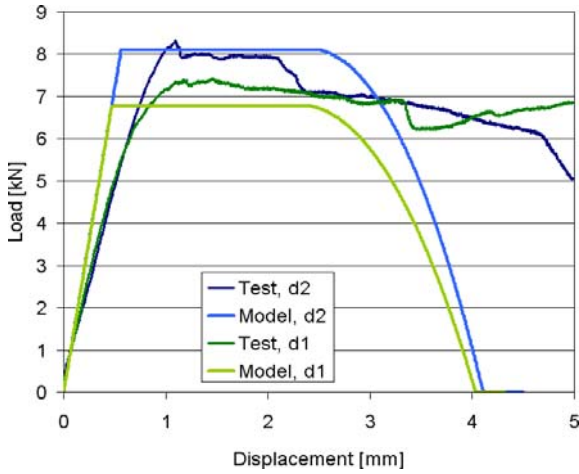


Fig 24. PLINK simulated shear force-displacement versus experimental trend for PH fasteners, $t1$.

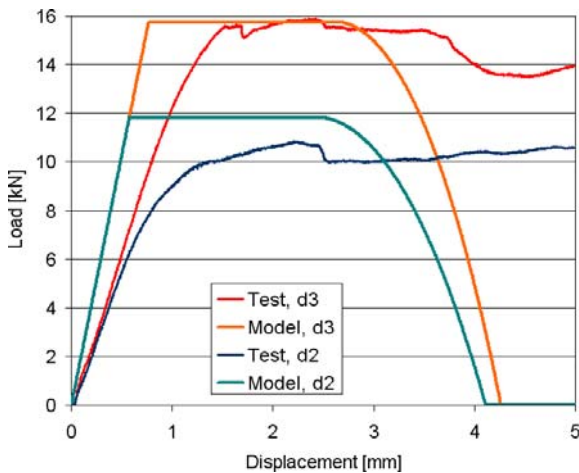


Fig 25. PLINK simulated shear force-displacement versus experimental trend for PH fasteners, $t2$.

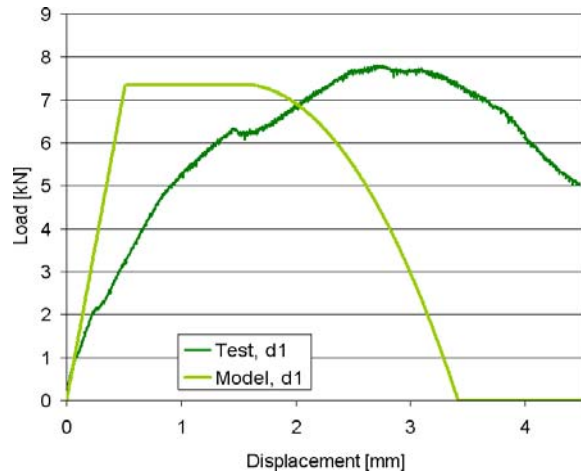


Fig 26. PLINK simulated shear force-displacement versus experimental trend for CS fasteners, $t1$.

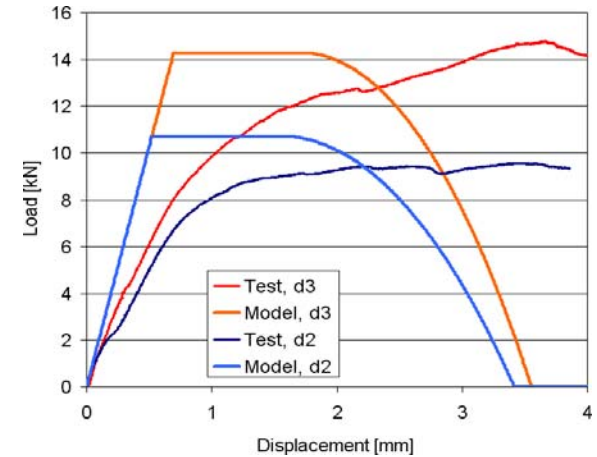


Fig 27. PLINK simulated shear force-displacement versus experimental trend for CS fasteners, $t2$.

4.4.3 Discussion

It can be seen from Figures 24-27 that the shear behaviour of the PLINK model is not as good as for the pull-through model, however the model still performs reasonably well up to the point of failure corresponding to D1. The variation in the ultimate load is a reflection of the variation in σ_{Su} for each specimen from the average value which was used to determine S_u for each specimen model.

In addition to the mesh dependency described in Section 5.4.1, another limitation of the PLINK model is that independent D1 and D2 values cannot be defined for shear and normal modes. It can be seen by comparison

with the shear test results that the simulation consistently under-predicts the area described by the load-displacement curves. It is clear from the testing that the displacement parameters D1 and D2 should be much larger for the shear loading than for pull-through, however the model does not allow this. It also would not be reasonable to average D1 and D2 values from the two different failure modes because these displacements can reach very high values under shear load.

6 Conclusion

A method for modelling composite fastened joints for crash and impact simulation has been developed around the PLINK element in Pam-Crash. A test program was devised and conducted that encompassed pull-through and shear loading on a range of different laminate thicknesses, fastener diameters and head types. Material parameters independent of laminate thickness and fastener size were calculated. These results were then used to simulate the test program and compare the model behaviour with that of the experiment. It was found that the PLINK model can provide a reasonably accurate and convenient method for modelling fastened composite joints for crash and impact simulations.

The biggest benefit of the PLINK model for this application is that they provide a mesh-independent and relatively-simple way to model fasteners. The biggest limitation found from this investigation was the inability to de-couple the normal and shear failure modes, particularly the displacements associated with ultimate failure and unloading.

In this analysis, the lowest strengths associated with pull-through and shear bearing failure modes were attributed to the PLINK element. Whilst this approach provides a simple method for modelling fastened joints in large structures, it must be remembered that failure of a PLINK actually reflects damage that has developed in one or more composite components, not failure of the fastener itself. This damage may not be reflected in the shell

elements connected by the PLINK. In future, this could be addressed by developing a joint element that has elements in the composite layers as well as representing the fastener. However, as the representation becomes more complex, so too does the modelling effort required to implement it, which must always be kept in balance with the aim of the simulation and other limitations of the analysis. For many contexts, the method for modelling composite fastened joints with the current PLINK as described in this paper is sufficient.

7. Recommendations

Several areas for further investigation are highlighted through this investigation:

- Test unidirectional tape and other composite materials to determine whether the failure mechanisms are similar.
- Investigate combined loading failure to improve understanding of how they interact and what the weighting factors should be, if indeed the modes should be coupled.
- Further investigate the unload-reload behaviour of both the joints and the model to understand the behaviour of both.
- Investigate the strength of composite fastened joints at high strain rates representative of crash and impact scenarios.

Acknowledgements

The authors would like to acknowledge the support of Pacific ESI and the German Aerospace Centre (DLR) who are contributing to the model development and experimental components of this on-going research program. The assistance of technical officers from RMIT University is gratefully acknowledged for their contribution to the quasi-static shear testing. The authors thank the support of Landesstiftung Baden-Wuerttemberg for scholarship funding of Hannes Körber. FE modelling assistance of Thomas Breitweg from the University of Stuttgart is gratefully acknowledged.

References

- [1] Ubels LC, Johnson AF, Gallard JP and Sunaric M, Design and testing of a composite bird strike resistant leading edge. *National Aerospace Laboratory (NLR)*, NLR-TP-2003-054, 2003.
- [2] McCarthy MA, Xiao JR, Petrinic N, Kamoulakos A and Melito V, Modelling of Bird Strike on an Aircraft Wing Leading Edge Made from Fibre Metal Laminates – Part 1: Material Modelling, *Applied Composite Materials*, Vol. 11, pp. 295-315, 2004.
- [3] McCarthy MA, Xiao JR, McCarthy CT, Kamoulakos A, J Ramos, Gallard JP and Melito V, Modelling of Bird Strike on an Aircraft Wing Leading Edge Made from Fibre Metal Laminates – Part 2: Modelling of Impact with SPH Bird Model, *Applied Composite Materials*, Vol. 11, pp. 317-340, 2004.
- [4] Banbury A and Kelly DW, A study of fastener pull-through failure of composite laminates. Part 1: Experimental, *Composite Structures*, Vol 45, pp. 241-254, 1999.
- [5] Langrand É, Deletombe É, Markiewicz and Pascal Drazétic, Numerical approach for assessment of dynamic strength for riveted joints, *Aerospace Science and Technology*, Vol 3, pp. 431–446, 1999.
- [6] Baker A, Dutton S, Kelly D, *Composite Materials for Aircraft Structures*, Second Edition. Blacksburg, Virginia : AIAA 2004
- [7] McCarthy MA, *BOJCAS: Bolted Joints in Composite Aircraft Structures*. Air & Space Europe Vol. 3 No 3/4, 2001.
- [8] *Pam-Crash Solver Reference Manual*, ESI Group, 2004
- [9] *Pam-Crash Solver Notes Manual*, ESI Group, 2004.
- [10] Niu MCY, *Airframe Structural Design, Practical Design Information and Data on Aircraft Structures*. Hong Kong : Conmilit Press Ltd. 1988
- [11] Banbury A, Kelly DW, Jain LK, A study of fastener pull-through failure of composite laminates. Part 2: Failure prediction. *Composite Structures* 45, pp 255-270, 1999
- [12] *MIL-HDBK-17-1E : Polymer Matrix Composites, Volume 1*. Guidelines for Characterization of Structural Materials. Department of Defense, USA (1994)
- [13] ASTM standard D5961/D5961M-05. Standard Test Method for Bearing Response of Polymer Matrix Composite Laminates, ASTM International 2005